AMERICAN SOCIETY FOR MICROBIOLOGY | Journal of Virology

Differential Control of BST2 Restriction and Plasmacytoid Dendritic Cell Antiviral Response by Antagonists Encoded by HIV-1 Group M and O Strains

Mariana G. Bego,[a] Lijun Cong,[a] Katharina Mack,[b] Frank Kirchhoff,[b] Éric A. Cohen[a,c]

Institut de Recherches Cliniques de Montréal (IRCM), Montreal, Quebec, Canada[a]; Institute of Molecular Virology, Ulm University Medical Center, Ulm, Germany[b]; Department of Microbiology, Infectiology and Immunology, Université de Montréal, Montreal, Quebec, Canada[c]

ABSTRACT

BST2/tetherin is a type I interferon (IFN-I)-stimulated host factor that restricts the release of HIV-1 by entrapping budding virions at the cell surface. This membrane-associated protein can also engage and activate the plasmacytoid dendritic cell (pDC)-specific immunoglobulin-like transcript 7 (ILT7) inhibitory receptor to downregulate the IFN-I response by pDCs. Pandemic HIV-1 group M uses Vpu (M-Vpu) to counteract the two BST2 isoforms (long and short) that are expressed in human cells. M-Vpu efficiently downregulates surface long BST2, while it displaces short BST2 molecules away from viral assembly sites. We recently found that this attribute is used by M-Vpu to activate the BST2/ILT7-dependent negative-feedback pathway and to suppress pDC IFN-I responses during sensing of infected cells. However, whether this property is conserved in endemic HIV-1 group O, which has evolved Nef (O-Nef) to counteract specifically the long BST2 isoform, remains unknown. In the present study, we validated that O-Nefs have the capacity to downregulate surface BST2 and enhance HIV-1 particle release although less efficiently than M-Vpu. In contrast to M-Vpu, O-Nef did not efficiently enhance viral spread in T cell culture or displace short BST2 from viral assembly sites to prevent its occlusion by tethered HIV-1 particles. Consequently, O-Nef impairs the ability of BST2 to activate negative ILT7 signaling to suppress the IFN-I response by pDC-containing peripheral blood mononuclear cells (PBMCs) during sensing of infected cells. These distinctive features of BST2 counteraction by O-Nefs may in part explain the limited spread of HIV-1 group O in the human population.

IMPORTANCE

The geographical distributions and prevalences of different HIV-1 groups show large variations. Understanding drivers of distinctive viral spread may aid in the development of therapeutic strategies for controlling the spread of HIV-1 pandemic strains. The differential spread of HIV-1 groups appears to be linked to their capacities to antagonize the long and short isoforms of the BST2 restriction factor. We found that the endemic HIV-1 group O-encoded BST2 antagonist Nef is unable to counteract the restriction mediated by short BST2, a condition that impairs its ability to activate ILT7 and suppress pDC antiviral responses. This is in contrast to the pandemic HIV-1 group M-specified BST2 countermeasure Vpu, which displays a diverse array of mechanisms to counteract short and long BST2 isoforms, an attribute that allows the effective control of pDC antiviral responses. These findings may help explain the limited spread of HIV-1 group O as well as the continued predominance of HIV-1 group M throughout the world.

BST2/tetherin is a type I interferon (IFN-I)-inducible surface protein with an unusual topology. The protein consists of a N-terminal cytosolic tail followed by a transmembrane domain (TMD) and an ectodomain that is membrane associated through a C-terminal glycosylphosphatidylinositol (GPI) anchor (1). BST2 inhibits the release of a broad array of enveloped viruses, including human immunodeficiency virus (HIV), by tethering budding virions to the surface of infected cells (2, 3). While the physical retention of progeny virions by BST2 was proposed to be a major obstacle limiting the initial local viral propagation needed for efficient transmission between individuals (4–6), increasing evidence indicates that this activity also has multiple immunological consequences that could restrict viral transmission fitness. Virion tethering by BST2 can sensitize infected cells to antibody (Ab)-dependent cell-mediated cytotoxicity (ADCC) (7–9) as well as activate proinflammatory NF-κB signaling via a dual-tyrosine motif in the cytoplasmic tail of the protein (10). Moreover, the physical limitation of HIV-1 particle release by BST2 was found to stimulate IFN-I production by plasmacytoid dendritic cells (pDCs) in the context of cell contacts between HIV-1-producing cells and pDCs (11). In this regard, BST2 can act as a ligand of immunoglobulin-like transcript 7 (ILT7), a pDC-specific inhibitory receptor that downregulates Toll-like receptor 7/9 (TLR7/9)-mediated IFN-I production upon pDC activation (11, 12). Mechanistic evidence suggests that virion tethering interferes with the ability of BST2 to act in conjunction with ILT7 as a negative regulator of the IFN response by pDCs (11).

Received 10 June 2016 **Accepted** 29 August 2016

Accepted manuscript posted online 31 August 2016

Citation Bego MG, Cong L, Mack K, Kirchhoff F, Cohen EA. 2016. Differential control of BST2 restriction and plasmacytoid dendritic cell antiviral response by antagonists encoded by HIV-1 group M and O strains. J Virol 90:10236–10246. doi:10.1128/JVI.01131-16.

Editor: G. Silvestri, Emory University

Address correspondence to Éric A. Cohen, eric.cohen@ircm.qc.ca.

HIV-1 is divided into four distinct groups (groups M, N, O, and P), which represent independent cross-species transmissions of a simian immunodeficiency virus (SIV) to humans (13). It is thought that the viruses resulting from these transmissions have spread with different efficiencies in the human population in part because of their differential adaption to human BST2 restriction (14). The SIV precursors of all HIV-1 groups and HIV-2 utilize the Nef accessory protein to antagonize BST2 from their respective primate hosts (6, 15, 16). However, a 5-amino-acid deletion in the cytoplasmic domain of human BST2 confers resistance to SIV Nef proteins. This species barrier is believed to have led the predominant HIV-1 group M and, less effectively, the minor group N strains to adapt and use Vpu to antagonize BST2 (6, 17), while HIV-2 adopted the envelope (Env) glycoproteins as a BST2 countermeasure (18). Although initial studies failed to identify a human BST2 viral antagonist in HIV-1 groups O and P (6, 19, 20), recent evidence reveals that HIV-1 O Nef can counteract human BST2, thus providing a potential explanation for the epidemic spread of HIV-1 group O in western central Africa (21, 22).

Two isoforms of human BST2 capable of restricting HIV-1 virion release have been described. They are derived from alternative translation initiation from two highly conserved methionine residues located in the cytoplasmic tail of the molecule (23). The short isoform lacks the first 12 N-terminal residues present in the long isoform, including conserved tyrosine and serine-threonine motifs. These isoforms have the ability to form homodimers and heterodimers, and while they display differential signaling activities (signaling is restricted to the long BST2 homodimer), they are all capable of interacting with ILT7 on pDCs (11). Primate lentivirus antagonists counteract BST2 restriction via intracellular sequestration, degradation, and/or displacement mechanisms to remove BST2 from sites of virus budding (24). The mechanisms differ significantly among the different viral countermeasures and according to the BST2 isoforms being targeted. For instance, both isoforms of human and rhesus macaque BST2 demonstrate similar sensitivities to HIV-2 Env and SIVmac Nef, respectively, and their counteraction involves the removal of the protein from the cell surface through enhanced internalization and intracellular sequestration (18, 25–27). The Vpu protein from the recently isolated highly pathogenic HIV-1 group N strain from Togo (N1.FR.2001) (17) also antagonizes both isoforms albeit without inducing their degradation or surface downregulation (28). In contrast, HIV-1 group M Vpu (M-Vpu) targets the long and short BST2 isoforms differentially using distinct mechanisms. While M-Vpu removes long BST2 molecules from the cell surface essentially via intracellular sequestration and degradation mechanisms, the short BST2 isoform is more resistant to M-Vpu-mediated downregulation and antagonism (23, 28) and, as such, appears to be counteracted by displacement from sites of virus budding (11, 29–31). Interestingly, the ability of M-Vpu to displace residual BST2 molecules away from sites of virus budding was found to have a downregulatory role in the pDC IFN-I response since it promoted the engagement of BST2 with the ILT7 inhibitory receptor upon cell contacts between infected cells and pDCs (11). Thus, differential targeting of long and short BST2 isoforms seems to be a specific property of HIV-1 M-Vpu (23, 28) and appears to be intended as a means to counteract BST2 restriction upon HIV-1 particle release, prevent the activation of NF-κB signaling, and limit IFN-I production by pDCs upon sensing of infected cells.

HIV-1 group O Nef proteins (O-Nefs) counteract human BST2 by targeting a domain in the N-terminal cytosolic region that is directly adjacent to the deleted residues that normally provide sensitivity to Nef. However, this domain is not present in short BST2, and as a result, O-Nefs can antagonize only the long BST2 isoform. Mechanistically, O-Nef, like M-Vpu, traps BST2 in the *trans*-Golgi network; although O-Nef slightly increases BST2 internalization, it is as efficient as M-Vpu in inhibiting BST2 anterograde transport to the cell surface (21). Interestingly, while Nef from the inferred group O most recent common ancestor (O-MRCA) was found to suppress BST2-mediated NF-κB activation almost as efficiently as the prototypical group M NL4.3 Vpu protein, this function appeared to be lost in contemporary HIV-1 group O *nef* alleles. Instead, contemporary O-Nefs, like contemporary Nef proteins from HIV-1 group M (M-Nefs), are unable to prevent NF-κB activation (21).

To define the functional consequences of the evolutionary adaptation of O-Nef to counteract BST2, we studied its fitness compared to that of M-Vpu in terms of its capacity to promote HIV-1 particle release and facilitate viral spread in $CD4^+$ T cells *in vitro*. In addition, we analyzed the ability of O-Nef to exclude BST2 from sites of viral assembly and activate the ILT7 inhibitory receptor as a means to evade the IFN-I response by pDCs. The data presented in this study show that BST2 antagonists encoded by pandemic HIV-1 group M and endemic HIV-1 group O differentially control the pDC antiviral response despite their shared capacity to counteract BST2 restriction of HIV-1 release.

MATERIALS AND METHODS

Antibodies and reagents. Rabbit polyclonal anti-BST2, anti-Vpu, anti-Nef, and anti-p17 Abs were previously described (32–35). Anti-ILT7 coupled with Alexa Fluor 647 was purchased from BioLegend. All secondary Abs used for flow cytometry and Western blotting were purchased from Life Technologies and Bio-Rad, respectively. Human recombinant interferon alpha 2a (rIFN-α2a) was purchased from PBL. Raltegravir was obtained through the NIH AIDS Reagent Program, Division of AIDS, NIAID, NIH.

Cell lines and plasmids. SupT1 and MT4 T cells were obtained from the NIH AIDS Reagent Program (36), and HEK293T cells were acquired from the ATCC, while HEK-blue human IFN reporter cell lines were purchased from InvivoGen. HEK293T cells were transiently transfected by using Lipofectamine 2000 (Invitrogen, Inc.). SupT1 cells stably expressing the short BST2 isoform (SupT1 ShortBST2) were established by lentiviral vector transduction based on pLenti-CMV/TO_Puro_DEST plasmids, as previously characterized (11). MT4 T cells transduced with a lentiviral vector encoding short hairpin RNA (shRNA) targeting BST2 (clone TRCN0000107018; OpenBiosystem) or control shRNA (target sequence 5′-CAACAAGATGAAGAGCACCAA-3′) were previously described and characterized (11).

The cell line CT550 (also known as ILT7 NFAT-GFP reporter cell line) was a generous gift from Yong-Jun Liu (37). In this reporter mouse cell line, which expresses ILT7 and FcεRIγ, green fluorescent protein (GFP) is driven by a nuclear factor of activated T cells (NFAT) promoter (NFAT-GFP) and results in GFP expression in response to ILT7 surface ligation.

The NL4.3-derived proviral constructs used in this study were previously described (21). Replication-competent NL4.3 proviral constructs encoding M-MRCA or N-MRCA Nef variants were generated by transferring HpaI-MluI fragments from NL4.3 dU Env-M-MRCA Nef_ires_GFP or NL4.3 dU Env-N-MRCA Nef_ires_GFP proviral constructs (previously described in reference 21), respectively, into NL4.3 dU Nef_ires_GFP. The sequences of the Vpu and Nef regions of all provirus constructs used were validated by automated sequencing. The plasmid encoding BST2 (pcDNA_Tetherin) was previously described (33).

HIV-1 production and infections. Infectious GFP-marked HIV-1 NL4.3 constructs with or without vesicular stomatitis virus glycoprotein (VSVg) were generated by Lipofectamine transfection of HEK293T cells. Virus-containing supernatants were harvested at 2 days posttransfection, clarified, pelleted by ultracentrifugation, and titrated by using TZM-bl indicator cells as described previously (33). T cells were infected with the different GFP-expressing pNL4.3 viruses at different multiplicities of infection (MOIs) ranging from 0.005 to 0.05. Infection rates were calculated by measurement of GFP-positive (GFP^+) cells by flow cytometry, as previously described (11).

Virus particle release assay. The release of virus particles was assessed by Western blotting as described previously (38). Viral particle release efficiency was evaluated by determining the ratio of the virion-associated Gag (p24) signal over the total intracellular Gag (p24 plus p55) signal measured by scanning densitometry analysis of Western blots. Viral release efficiency was normalized to the value obtained from cells infected with the wild-type (WT) virus, which was set at 100%.

Surface antigen staining and flow cytometry analysis. Cell surface BST2 staining and flow cytometry analysis of live cells were performed as previously described (33). Samples were analyzed by using a Cyan flow cytometer with FlowJo software (TreeStar).

Confocal microscopy. Primary $CD4^+$ T cells and MT4 and SupT1 cell lines were infected with NL4.3 viruses. VSVg-pseudotyped viruses were used for infection of primary $CD4^+$ T cells. MT4 T cells were infected in the presence of raltegravir to limit infection to a single round of replication (25 ng/ml of raltegravir was added at 8 h postinfection [hpi]). At 48 h postinfection, T cells were immunostained with anti-BST2 Abs at 4°C for 45 min prior to extensive washes. Cells were then plated onto poly-D-lysine-treated coverslips and fixed for 30 min in 4% paraformaldehyde (PFA). Viral matrix p17, a product of Gag polyprotein processing by the viral protease, was used as a marker of assembling HIV-1 particles and was detected with a specific antibody that does not recognize immature Gag products (34). To detect p17, fixed cells were permeabilized in 0.2% Triton for 5 min, incubated for 2 h at 37°C in 5% milk–phosphate-buffered saline (PBS) containing anti-p17 Abs, washed, and incubated with the appropriate secondary Ab for 30 min at room temperature. All analyses were conducted by using a 63× Plan Apochromat oil immersion objective with an aperture of 1.4 on an LSM710 Observer Z1 laser scanning confocal microscope coupled with a Kr-Ar laser (Zeiss). Signals from assembling viral particles stained with anti-p17 or from surface BST2 were quantified by measuring the raw integrated signal density on manually selected cells using ImageJ software.

Preparation of PBMCs and primary $CD4^+$ T cells. Peripheral blood samples were obtained from healthy adult donors who gave written informed consent in accordance with the Declaration of Helsinki under research protocols approved by the research ethics review board of the Institut de Recherches Cliniques de Montréal (IRCM). Peripheral blood mononuclear cells (PBMCs) were isolated by Ficoll-Paque centrifugation (GE Healthcare) and cultured in RPMI 1640 medium supplemented with 10% fetal bovine serum (FBS). $CD4^+$ T lymphocytes were isolated by negative selection using a $CD4^+$ T cell isolation kit (Miltenyi Biotec). Enriched $CD4^+$ T cells were then activated by using phytohemagglutinin-L (PHA-L; 5 μg/ml) for 48 h and maintained in complete RPMI 1640 medium supplemented with interleukin-2 (IL-2) (100 U/ml). Activated primary T cells were infected at 5 days postisolation.

Coculture assay with PBMCs. Two days prior to coculture, T cells were infected with the different GFP-expressing pNL4.3 viruses at different MOIs. Infection rates were calculated by measurement of GFP^+ cells by flow cytometry, as previously described (11). Briefly, cultures with a range of 20 to 50% infected cells were subsequently used for cocultures. Target and donor cells were mixed at a ratio of 3:1 (PBMCs to T cells) in a final volume of 250 μl and cultured in U-bottom 96-well plates for 18 to 22 h. Cocultures were then transferred to a V-bottom 96-well plate and centrifuged for 5 min at 400 × *g*. Supernatants were then used to quantify the amounts of IFN-I produced. Each experimental replicate was performed by using cells from a different donor.

Quantification of IFN-I concentrations. Detection of bioactive human IFN-I was performed by using the reporter cell line HEK-Blue IFN-α/β (InvivoGen) as previously reported (39). The IFN-I concentration (units per milliliter) was extrapolated from the linear range of a standard curve generated using known amounts of IFN-I.

Activation of ILT7 using $ILT7^+$ NFAT-GFP reporter cells. HEK293T cells were mock transfected or cotransfected with a BST2-encoding plasmid and GFP-expressing HIV proviruses (50,000 cells/well) and plated onto 24-well plates for 18 to 24 h. The following day, $ILT7^+$ NFAT-GFP reporter cells (100,000 cells/well) were added, and cocultures were incubated for an additional 18 to 24 h at 37°C, at which time samples were collected and analyzed by flow cytometry for BST2, ILT7, and GFP expression. HEK293T and NFAT-GFP reporter cells can be distinguished by flow cytometry based on their overall size and morphology (side scatter and forward scatter) as well as by monitoring ILT7 expression on reporter cells. The HEK293T cell transfection efficiency was determined in ILT7-negative cells as the percentage of cells expressing both GFP and surface BST2. Activation of ILT7 reporter cells was determined as the percentage of $ILT7^+$ cells that were GFP^+.

Statistical analysis. Statistical analysis was performed by using repeated-measures or one-way analysis of variance (ANOVA) with Bonferroni's multiple-comparison test or two-tailed paired Student's *t* tests, as indicated. A P value of <0.05 was considered significant.

RESULTS

Group O Nef enhances HIV-1 particle release and downmodulates surface BST2 but does not accelerate viral spread. To examine the effect of O-Nefs on the BST2 restriction exerted on HIV-1 particle release and spread, we used previously characterized replication-competent GFP-marked NL4.3 derivatives encoding different O-Nefs in a Vpu-defective (dU) background. Two O-Nefs were selected: the O-MRCA and primary isolate HJ162 (21). First, MT4 T cells were infected with the same NL4.3-derived viruses, and similar percentages of infected cells (~30% GFP^+ cells) were analyzed for HIV-1 release and surface BST2 downmodulation. Even in the context of viral infection, O-Nefs were capable of counteracting the restriction imposed on viral particle release by BST2 (Fig. 1A and B), and this effect correlated with a reduction of BST2 levels at the cell surface (Fig. 1C and D). NL4.3 Vpu was more effective at enhancing HIV particle release than O-Nefs during infection of MT4 T cells (Fig. 1A and B). Next, the kinetics of viral spread in MT4 cells expressing or not expressing BST2 were studied (Fig. 2A). Viral spread assays initiated at a low MOI revealed that the WT NL4.3 virus disseminated more rapidly than did Vpu-deficient viruses expressing O-Nefs, consistent with the fact that O-Nef-expressing viruses displayed less-effective antagonism toward BST2 (Fig. 1 and 2B). Depletion of BST2 in MT4 cells abolished the differential kinetics of viral spread observed between Vpu-expressing viruses and those deficient for Vpu but expressing O-Nef, indicating that this effect was entirely BST2 dependent (Fig. 2C). Two recent reports identified the cellular serine incorporator (SERINC) proteins SERINC3 and SERINC5 as potent inhibitors of HIV-1 particle infectivity, which are counteracted by HIV-1 Nef (40, 41). Therefore, the positive effect of M-Nef on virus infectivity and spread is restricted to cells expressing SERINCs, a group that does not include MT4 cells (41). Consequently, due to the lack of anti-BST2 activity of M-Nef and the absence of SERINC expression in MT4 cells, viruses lacking both Vpu and Nef behaved very similarly to viruses lacking Vpu but expressing M-Nef (40, 41). Overall, these results suggest that

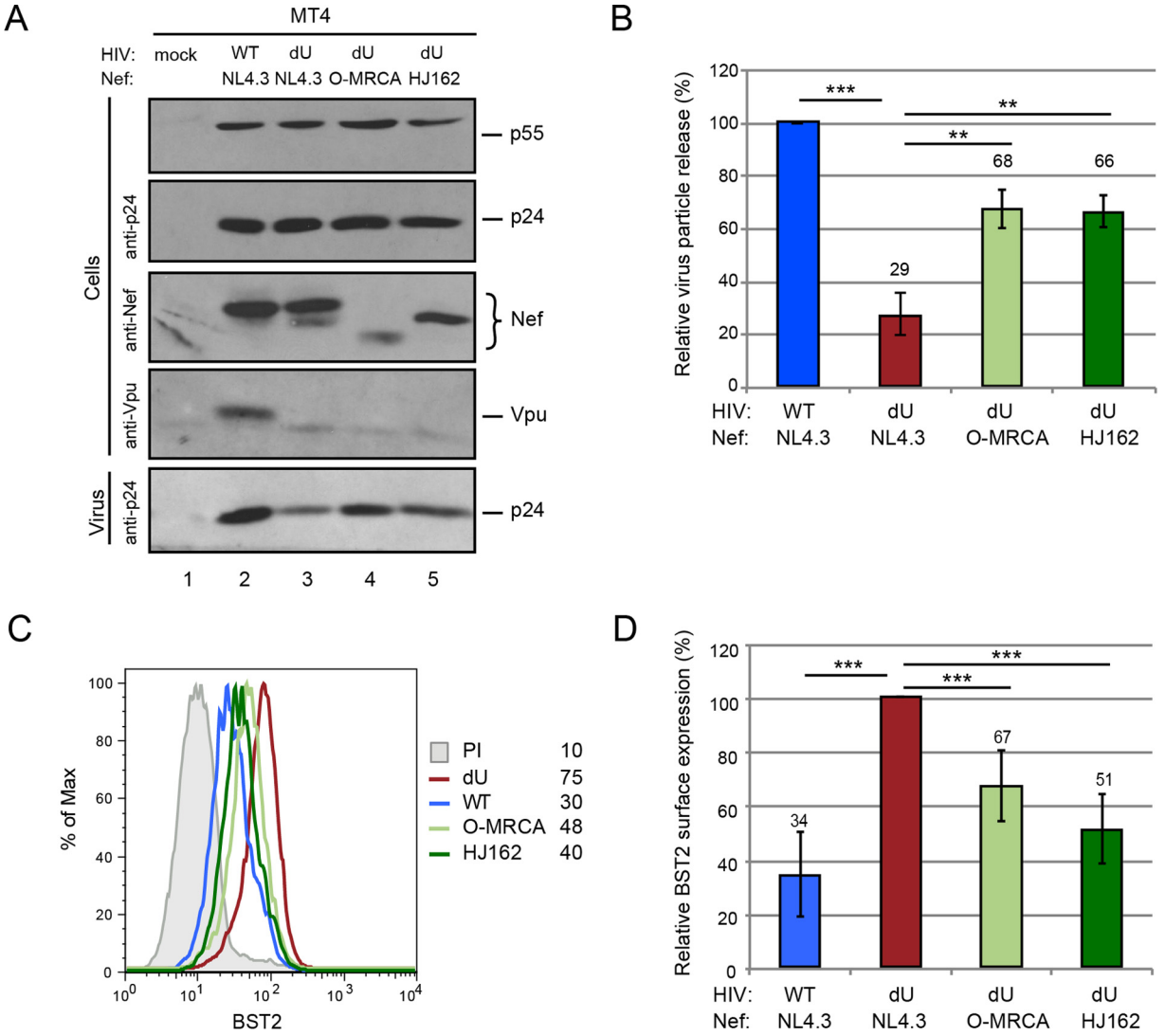

FIG 1 Group O Nefs retain some BST2 antagonism. (A and B) MT4 T cells were mock infected or infected with GFP-expressing NL4.3 WT and dU viruses expressing either NL4.3 Nef or O-Nefs, as indicated. Infected cell populations with ~30% GFP^+ cells at 48 hpi were selected for comparison. (A) Cells and virion-containing supernatants were analyzed for the presence of Gag, Nef, and Vpu proteins by Western blotting. (B) The relative virus particle release efficiency was calculated as described in Materials and Methods and normalized to the value obtained for the WT virus, which was set at 100% ($n = 3$). (C) Flow cytometry analysis of surface BST2 in GFP-positive MT4 T cells infected with the indicated viruses. Mean fluorescence intensity values are indicated for each sample (staining using preimmune rabbit serum [PI]). (D) Relative BST2 surface expression levels after infection with the indicated HIVs ($n = 4$). The percent mean fluorescence intensity values were calculated relative to dU HIV-producing cells (100%). A two-tailed paired *t* test was used (***, $P < 0.001$; **, $P < 0.01$). Error bars represent standard deviations.

although O-Nef variants have evolved some activity against human BST2, this activity does not appear to be sufficient to enhance the kinetics of viral dissemination at a low virus input, at least *in vitro*.

Group O Nef does not displace BST2 from sites of virus assembly. M-Vpu downmodulates a large proportion of long BST2 from the cell surface, while it excludes many of the remaining molecules (long BST2 remaining at the cell surface and Vpu downmodulation-resistant short BST2) from sites of viral assembly by virtue of its ability to target the BST2 TMD (11). Although HIV-1 O-Nef proteins efficiently reduce the cell surface expression of the long but not the short human BST2 isoform, it is unclear if they have the ability to displace BST2 away from virus assembly sites. To address this question, we evaluated the frequency of surface BST2 molecules that are not engaged in the restriction of progeny virions in the presence or the absence of O-Nefs. To this end, we performed colocalization studies of BST2 and HIV-1 Gag-p17, a marker of assembling HIV, on infected MT4 and primary $CD4^+$ T cells. T cells were infected with the above-described viruses and stained for surface BST2 and intracellular p17. As previously reported (11), clusters of BST2 molecules not colocalizing with p17 were detected on WT- but not on dU-infected MT4 and primary $CD4^+$ T cells, consistent with the ability of NL4.3 Vpu to displace a pool of surface BST2 away from virus assembly sites (Fig. 3A and B). Hence, in the absence of BST2 countermeasures, the majority of surface BST2 appears to be engaged in restricting assembling viruses. Indeed, consistent with the viral particle release data shown in Fig. 1A and B, significant

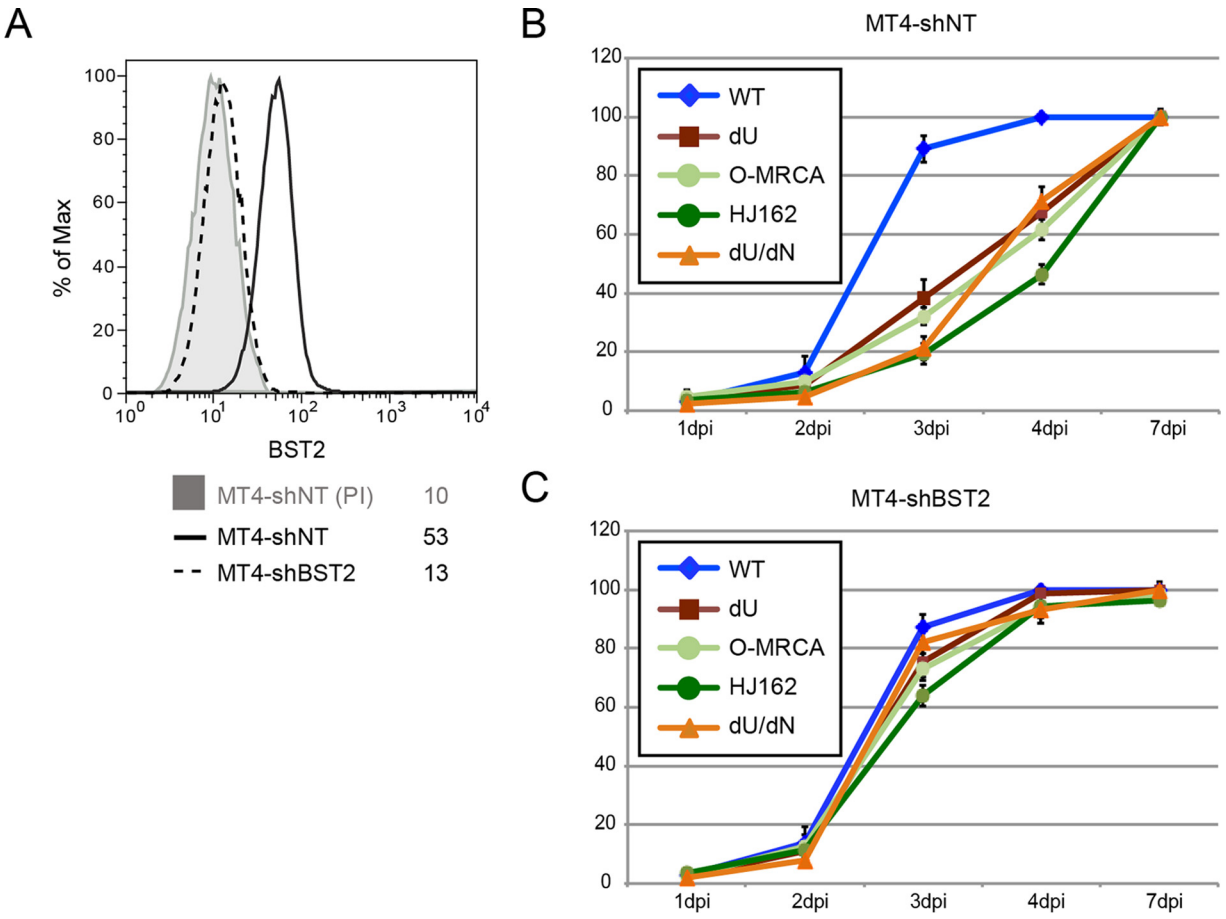

FIG 2 Group O Nefs cannot overcome BST2 restriction in viral spread assays. (A) Flow cytometry analysis of surface BST2 in control (MT4-shNT) or BST2-depleted (MT4-shBST2) cells. (B and C) MT4-shNT (B) and MT4-shBST2 (C) cells were infected with GFP-expressing NL4.3 WT and dU viruses expressing either no Nef (dN), NL4.3 Nef, or O-Nefs, as indicated ($n = 3$). A fraction of the cells was collected every day, and the percentage of GFP$^+$ cells was evaluated by flow cytometry. Error bars represent standard deviations.

accumulation of the MA signal, reflecting assembling viral particles, was detected in infected MT4 and primary CD4$^+$ T cells in the absence of BST2 countermeasures (Fig. 3C). While reduced levels of the MA signal were observed when either Vpu or O-Nefs were expressed, higher levels of the MA signal accumulated in the presence of O-Nef than in the presence of Vpu, reflective the less-effective BST2 antagonism of Nefs (Fig. 3C). As shown by the flow cytometry data in Fig. 1C and D, surface BST2 levels were significantly decreased in infected MT4 and primary CD4$^+$ T cells in the presence of M-Vpu and, to a lesser extent, O-Nefs (Fig. 3D). This reduction of surface BST2 levels correlated with decreased p17 accumulation at the cell periphery (Fig. 3A and C), the degree of which was commensurate with the increase in virus particle release observed in MT4 T cells (Fig. 1A and B). Interestingly, although the presence of O-Nefs reduced the levels of p17 detected at the cell periphery, the large majority of the remaining p17 localized perfectly with BST2. Indeed, no free BST2 was detected on cells infected with dU/O-Nef viruses (Fig. 3A and B), suggesting that in contrast to HIV-1 Vpu, O-Nef is unable to displace BST2 from virus budding sites.

Since Vpu is unable to downregulate and degrade the short BST2 isoform, yet can counteract it to some degree via displacement from virus assembly sites (11, 29), we next assessed if O-Nefs could affect the distribution of short BST2 isoforms relative to assembling virions. To this end, we used a SupT1 T cell line that expresses only this isoform of BST2 (SupT1 ShortBST2). Despite the lack of downregulation of the short isoform by Vpu (Fig. 3D), we did not observe a marked accumulation of p17 staining at the periphery of SupT1 ShortBST2 cells infected with WT viruses (Fig. 3A and C). This was in sharp contrast to dU- or O-Nef-expressing HIV-infected cells, which expressed similar levels of surface BST2 but displayed a noticeable accumulation of cell-associated p17 (Fig. 3A, C, and D). Consistent with our observations of MT4 and primary CD4$^+$ T cells, no significant amounts of free BST2 were detected in the absence of Vpu regardless of whether or not O-Nefs were expressed in infected SupT1 ShortBST2 cells (Fig. 3B). Overall, these results suggest that O-Nefs are unable to displace BST2 from sites of virus assembly.

Group O Nef is unable to suppress the production of IFN-I during innate sensing of HIV-1-infected cells. We previously postulated that BST2 molecules found outside sites of WT HIV assembly are free to bind and activate ILT7, a condition that reduces IFN-I production by pDCs upon contact with infected cells (11). Using ILT7$^+$ NFAT-GFP reporter cells that express GFP upon ILT7 activation (Fig. 4A), we previously found that Vpu-mediated BST2 antagonism generates a pool of surface BST2 mol-

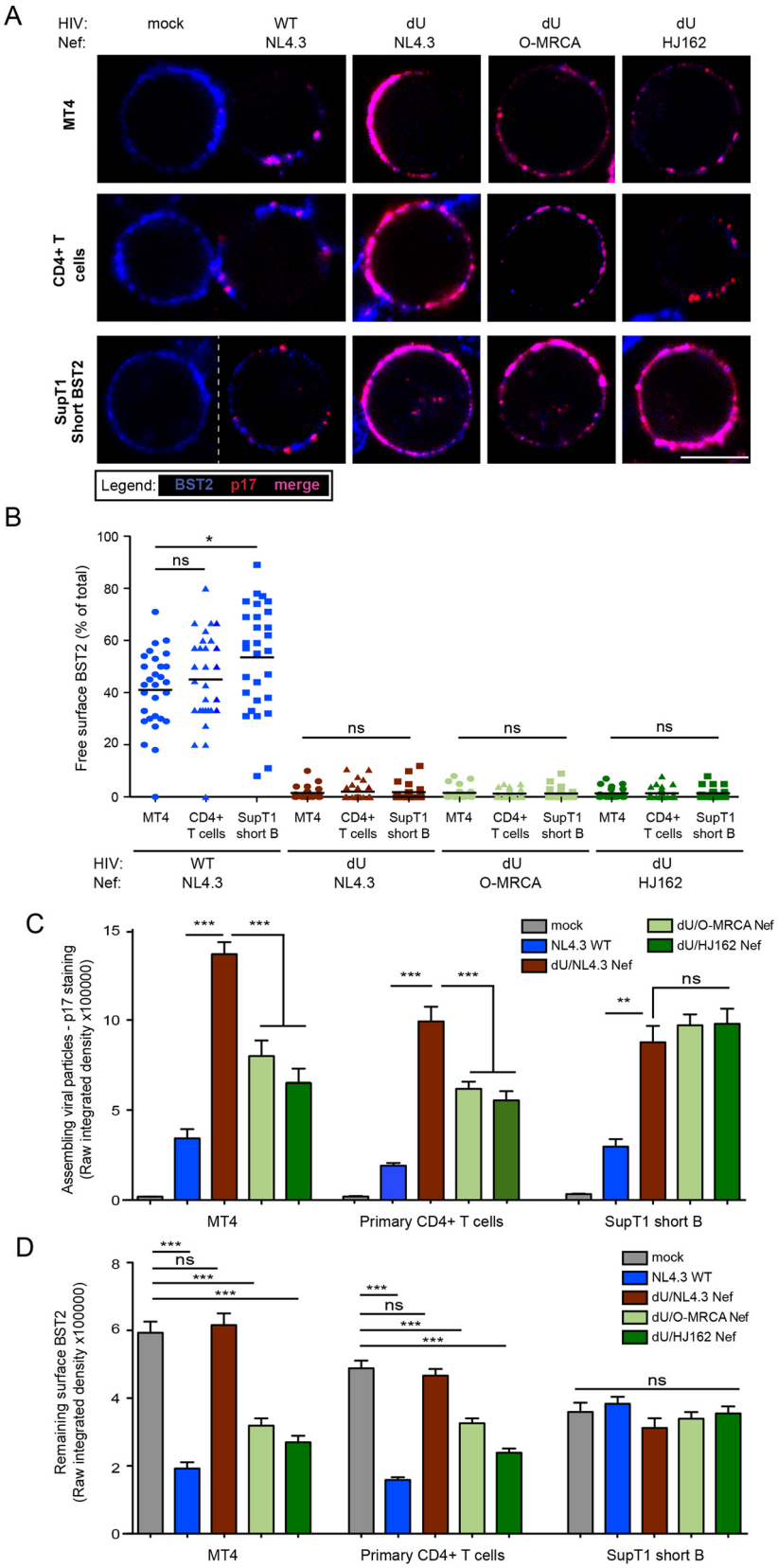

FIG 3 O-Nef, unlike M-Vpu, cannot displace BST2 from sites of virus assembly. MT4 cells, primary CD4$^+$ T cells, and SupT1 ShortBST2 cells were mock infected (mock) or infected with GFP-expressing NL4.3 WT and dU viruses expressing either NL4.3 Nef or O-Nefs, as indicated. (A) Cells were stained with anti-BST2 Abs, fixed, permeabilized, and then sequentially stained with anti-p17 Abs. An uninfected cell(mock) is shown next to WT-infected cells, as indicated. Bar = 10 μm. (B) The number of residual BST2 clusters not colocalizing with p17 (designated free BST2) per cell was calculated and expressed as the percentage of the total number of surface BST2 clusters. (C and D) The signal from assembling viral particles stained with p17 (C) or surface BST2 (D) was quantified by measuring the raw integrated signal density on manually selected cells using ImageJ software. Error bars indicate standard errors of the means after analysis of at least 50 distinct cells. One-way ANOVA with Bonferroni's multiple-comparison test was used (***, $P < 0.001$; **, $P < 0.01$; *, $P < 0.05$; ns, not significant [$P > 0.05$]).

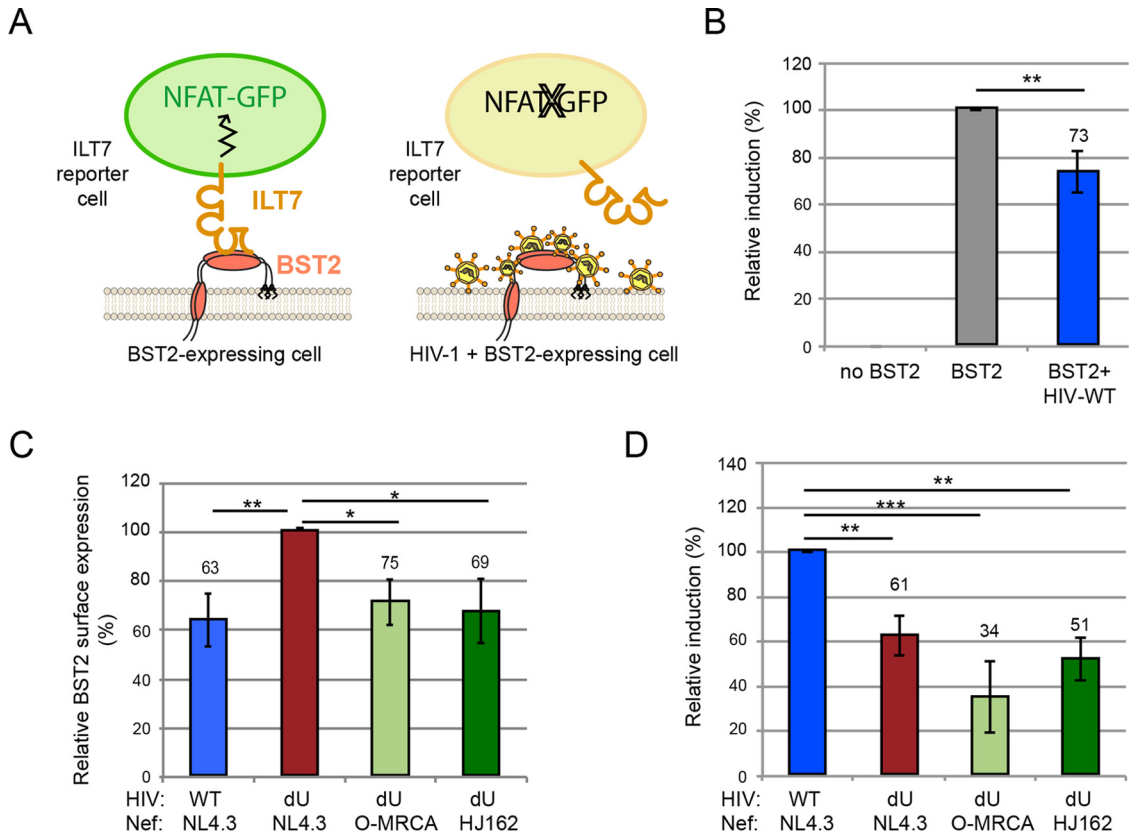

FIG 4 BST2 antagonism by group O Nefs does not lead to BST2-dependent activation of ILT7. (A) Schematic representation of the experimental ILT7 NFAT-GFP reporter coculture system. (B to D) ILT7$^+$ NFAT-GFP reporter cells were cocultured with control transfected HEK293T (no BST2) or BST2-expressing HEK293T (BST2) cells that were mock transfected or cotransfected with GFP-expressing NL4.3 WT and dU proviruses expressing either NL4.3 Nef or O-Nefs, as indicated. The degrees of surface BST2 downmodulation and ILT7 activation were determined by flow cytometry. ILT7 activation was evaluated as the percentage of GFP$^+$ reporter cells. (B) Percentage of ILT7 activation after coculture with the indicated HEK293T cells relative to BST2-expressing HEK293T cells (100%) ($n = 3$). (C) Relative BST2 surface expression levels in cells cotransfected with BST2 and the indicated HIV proviruses ($n = 3$). Percent mean fluorescence intensities were calculated relative to values for dU HIV-producing cells (100%). (D) Percentage of ILT7 activation after coculture with the indicated BST2-expressing HEK293T cells relative to WT NL4.3-producing HEK293T cells (100%) ($n = 3$). Repeated-measures ANOVA with Bonferroni's multiple-comparison test was used (***, $P < 0.001$; **, $P < 0.01$). Error bars represent standard deviations.

ecules capable of engaging and activating ILT7 upon cell-to-cell contact (11). To examine whether the presence of O-Nef in HIV-producing cells could affect ILT7 activation through BST2, we cocultured ILT7$^+$ NFAT-GFP reporter cells with control or BST2-expressing HEK293T cells cotransfected with our panel of pNL4.3 derivatives. While ILT7 activation was very effective in coculture with BST2-expressing cells, it was significantly reduced when these cells were coexpressing WT HIV, consistent with Vpu-mediated BST2 downmodulation (Fig. 3B and C). As previously reported (11), BST2$^+$ HEK293T cells expressing WT HIV activated ILT7 to a higher degree than did identical cells expressing dU HIV (Fig. 4D). Despite the ability of O-Nef to downregulate surface BST2 (Fig. 4C), BST2$^+$ HEK293T cells expressing dU/O-Nef HIV were the least potent activators of the ILT7 reporter cell line (Fig. 4D). In this context, it is expected that a large proportion of the remaining surface BST2 molecules are engaged in restricting progeny viruses, as shown in Fig. 3A.

We next examined the role of O-Nefs during innate sensing of infected T cells by PBMCs, a system where innate sensing and IFN-I production were almost entirely dependent on the presence of pDCs (11, 42). MT4 T cells were infected with GFP-encoding NL4.3 WT and dU viruses expressing M-Nefs (NL4.3) or O-Nefs. In these experiments, we also introduced a dU NL4.3 virus encoding Nef genes belonging to HIV-1 group M and N MRCAs. Infected MT4 T cell populations with a similar percentage of infected cells (GFP$^+$ cells) were cocultured with freshly isolated human PBMCs for 18 to 24 h, and the level of IFN-I production in the culture supernatant was measured (Fig. 5A). Consistent with previously reported results (11, 42), IFN-I was very efficiently detected only after coculture of infected T cells with PBMCs (Fig. 5B and C). Analysis of innate sensing of HIV-1-infected cells by PBMCs from different donors revealed that the presence of Vpu in infected donor cells led to a significant reduction of IFN-I production (Fig. 5C). In agreement with the lack of free surface BST2 potentially accessible for interaction with ILT7 in MT4 cells infected with dU virus expressing O-MRCA or contemporary Nefs (Fig. 3), no reduction of IFN-I production was observed when these infected cells were cocultured with PBMCs. Similar results were obtained when MT4 cells were infected with dU viruses expressing M-MRCA and N-MRCA Nef proteins (Fig. 5B and C), thus highlighting the lack of activity of these Nef variants.

Collectively, these results suggest that O-Nef cannot act in con-

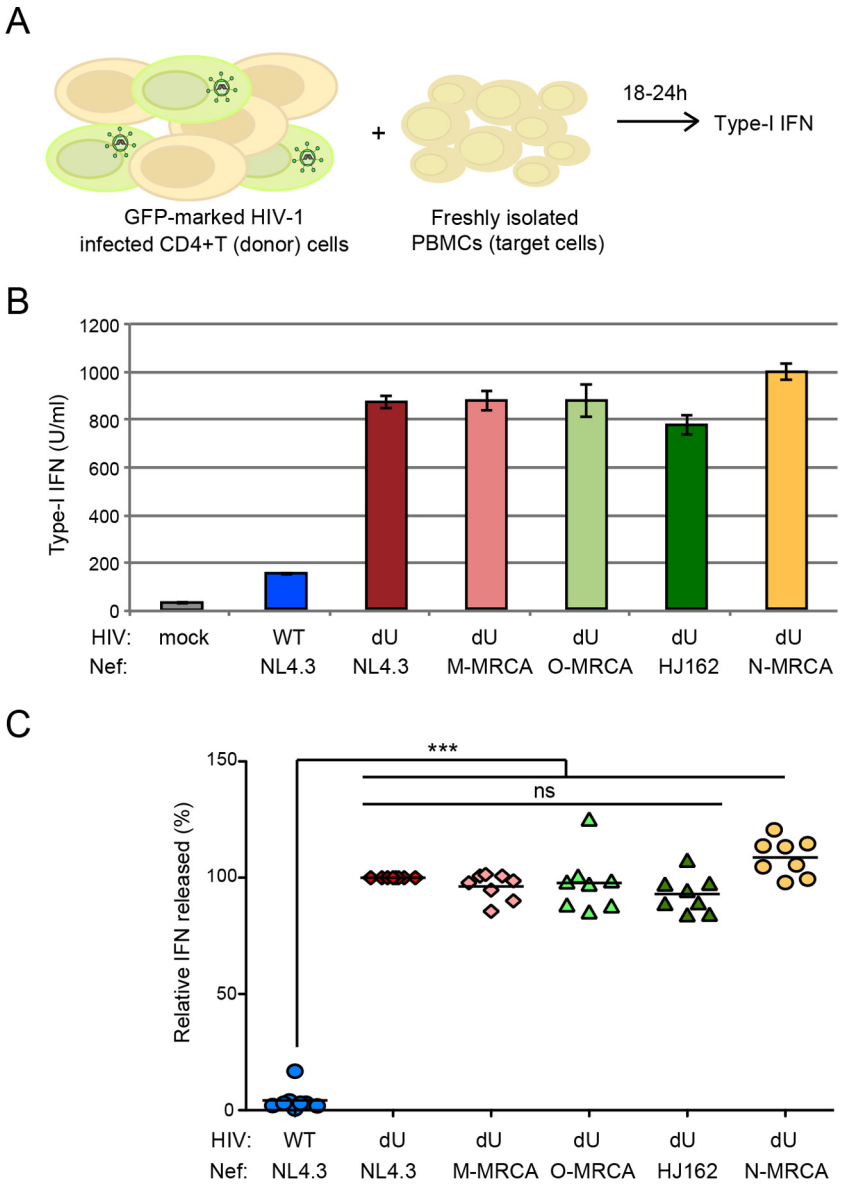

FIG 5 Group O Nefs cannot attenuate innate sensing of infected cells by pDC-containing PBMCs. (A) Schematic representation of the experimental system. WT or dU HIV-infected T cells were cocultured with freshly isolated PBMCs, and levels of bioactive IFN-I released into the supernatants were measured 18 to 24 h later. (B and C) MT4 T cells were mock infected or infected with GFP-expressing NL4.3 WT or dU viruses expressing either NL4.3 Nef, M-MRCA Nef, O-Nefs, or N-MRCA Nef, as indicated, and cell populations harboring similar percentages of infected T cells were cocultured with PBMCs. After 24 h of coculture, levels of IFN-I released into the supernatants were measured. Representative examples of absolute levels (B) and relative percentages (C) of IFN-I detected after coculture of HIV-1-infected MT4 donor cells with PBMCs ($n = 8$) are shown. The amount of IFN-I released by PBMCs in contact with dU/NL4.3 Nef-infected cells was set at 100%. Repeated-measures ANOVA with Bonferroni's multiple-comparison test was used (***, $P < 0.001$; ns, not significant [$P > 0.05$]). Error bars represent standard deviations.

junction with ILT7 to suppress the production of IFN-I triggered upon the sensing of HIV-1-infected cells by PBMCs. Indeed, O-Nef, unlike M-Vpu, is unable to displace BST2 from sites of virus budding and consequently cannot generate a pool of surface BST2 with the capacity to engage and activate ILT7 upon cell contacts between infected cells and pDCs.

DISCUSSION

Genetic and functional evidence strongly suggests that the ability of lentiviruses to counteract BST2 represents a critical property for viral transmission *in vivo* (6, 14). However, despite the fact that HIV-1 group O strains account for infections of 100,000 individuals, mostly in western central Africa (22), several reports suggested that these viruses failed to evolve an effective antagonist of human BST2 (6, 20). Recent functional analyses of group O Nef proteins in transient-expression model systems as well as in infected primary $CD4^+$ T cells revealed that HIV-1 group O strains have evolved the ability to counteract human BST2 through Nef (21). In the present study, we confirmed that HIV-1 group O MRCA and contemporary Nefs reduce the cell surface expression of BST2 and enhance virus particle release (Fig. 1). We further

show that despite having the capacity to mediate the release of significant amounts of virus, O-Nefs are unable to efficiently overcome the BST2 restriction imposed on viral spread in $CD4^+$ MT4 T cells at a low initial virus input (Fig. 2). In contrast to M-Vpu, O-Nefs do not appear to displace short BST2 away from sites of viral assembly, and as a result, cell surface BST2 molecules not colocalizing with assembling viruses (free BST2) are not detected at the surface of infected $CD4^+$ T cells (Fig. 3). Hence, O-MRCA and contemporary Nefs do not allow BST2-dependent activation of the pDC-inhibitory receptor ILT7 (Fig. 4) to suppress IFN-I production by pDCs during innate sensing of HIV-infected T cells (Fig. 5). Thus, in contrast to M-Vpu, O-Nefs are unable to activate the BST2/ILT7-dependent negative-feedback pathway that impedes the IFN-I response by pDCs. These distinctive features of BST2 counteraction by O-Nefs may play a role in the limited spread of HIV-1 group O strains in the human population compared to the predominant group M viruses.

Our data showing that O-Nefs downregulate human BST2 and enhance the release of virus particles in MT4 T cells are consistent with previously reported observations and indeed confirm that during adaptation to human hosts, O-Nefs have gained activity against human BST2. However, the degree to which it counteracted human BST2, as measured by surface BST2 downregulation or virus particle release, was reduced compared to that for Vpu. Indeed, our analysis of viral spread at a low virus input, a condition that likely reflects the environment prevailing during early stages following HIV transmission (the "eclipse period"), revealed that O-Nef-expressing viruses are spreading with reduced kinetics compared to those of Vpu-expressing viruses; in fact, their spread is more comparable to that of Vpu-defective viruses. These results suggest that despite the ability of O-Nef to enhance virus particles, the amounts of released viruses for cell-free virus transmission remain quantitatively limited in the initial rounds of infection. Kluge and colleagues (21) found that in primary $CD4^+$ T cells pretreated with type I IFN (which enhances surface BST2 levels and restriction), viruses expressing M-Vpu or O-Nef proteins replicated with near-identical kinetics and released very similar amounts of virus at late time points after infection. However, at early time points (3 days postinfection [dpi]), significantly less virus was produced from cultures infected with O-Nef-expressing viruses than from those infected with M-Vpu-expressing viruses. Thus, our findings in MT4 cells are consistent with the results of Kluge and colleagues in primary $CD4^+$ T cells except that the delay of O-Nef-expressing virus spread at early time points seems to be amplified in MT4 cells. Indeed, similar to our findings in MT4 cells lacking BST2, no significant difference in virus production was observed in the context of primary $CD4^+$ T cells infected with viruses expressing M-Vpu or O-Nef in the absence of type I IFN pretreatment, a condition where primary $CD4^+$ T cells express very low basal levels of BST2. Thus, O-Nefs appear to be less effective at overcoming BST2-dependent restriction of viral spread, especially under conditions where BST2 is highly expressed.

Group O strains emerged relatively early in the HIV pandemic, alongside group M, suggesting that this group had fair opportunities to disseminate, as group M did. Its limited spread among the population could be due to viral and/or host factors (43). Relative to group M, many infection parameters in HIV-1 group O-infected patients remain largely understudied. During prototypical disease progression in individuals infected with HIV-1 group M, neutralization escape variants are generated, and infecting CCR5 viruses (R5) switch tropism to CXCR4 (X4) or dual-tropic viruses. This change in tropism is followed by a marked depletion of $CD4^+$ T cells, an increase in the plasma viral load, and poor disease prognosis. Data from a small number of studied cases of group O infection suggest a disease course and pathogenesis similar to those reported previously for group M infection (44, 45). Nonetheless, tropism studies revealed a significant R5 prevalence even during late stages of infection (46). The coreceptor switch from R5 to X4 may be uncommon within this group and could imply that group O-infected patients potentially progress to disease more slowly than do group M-infected patients, and indeed, some of these patients could behave as long-term nonprogressors (47). HIV-1 group O is the least fit among all HIV types and groups. HIV-1 group M was found to be typically 100-fold more fit than group O in cell culture (48). The reduced replication and transmission fitness were proposed to be responsible for the low prevalence and limited geographical spread of HIV-1 group O in the human population. Whether the reduced transmission fitness of HIV-1 group O could be due in part to its limited capacity to overcome BST2, as shown by our *in vitro* observations, remains a reasonable possibility. Even though HIV-1 group O Nef is capable of facilitating virus particle release by targeting essentially long BST2 isoforms, it is unable to downregulate short BST2 molecules from the cell surface (21) or displace them from sites of viral assembly, as shown by our surface BST2-p17Gag colocalization studies. This attribute of O-Nef proteins may be responsible for the inefficient viral spread observed *in vitro* under conditions of limiting virus input. Previous studies using humanized mice suggested that BST2 antagonism by Vpu facilitated HIV-1 replication and propagation *in vivo*, in particular during early stages following infection, where transmission by cell-free virus may play a critical role (4, 5). In contrast to M-Vpu, O-Nef may not be effective at promoting the initial burst of viral proliferation and expansion that is most likely necessary to enable dissemination to local lymphoid tissues and the establishment of systemic infection (49).

pDCs constitute a major source of IFN-I production during acute HIV infection, and their activation results primarily from TLR7-mediated sensing of HIV-infected cells (11, 42, 50). We previously proposed a mechanism of innate immune evasion whereby M-Vpu mediates the activation of a BST2/ILT7-dependent negative-feedback pathway that normally impedes the IFN-I response when pDCs are activated (11). This mechanism is dependent on Vpu's ability to displace surface BST2 molecules, in particular the short isoforms, away from sites of viral assembly where they would be free to engage and activate the pDC-inhibitory receptor ILT7 upon cell-to-cell contacts. The mechanism of BST2 displacement by Vpu was shown to involve a physical association of the two proteins through their respective TMDs as well as a highly conserved dileucine sorting motif (ExxxLV, where *x* represents any amino acid) in the Vpu cytoplasmic domain capable of binding the major cellular clathrin adaptor proteins AP1 and AP2 (29, 31, 51, 52). Data from our surface BST2-p17Gag colocalization analysis suggest that the mechanism underlying human BST2 antagonism by O-Nefs does not involve a displacement of surface BST2 molecules from sites of virus budding, even though a highly conserved dileucine motif (ExxxLL) in O-Nef was found to be required for human BST2 counteraction (21). Thus, in contrast to Vpu, it appears that O-Nefs have not evolved any activity to counteract surface BST2 molecules that are resistant to downregulation, such as the short isoform. While short BST2 retains an intact

TMD required to bind Vpu, it lost the determinants required to bind O-Nef. Indeed, Kluge and colleagues mapped the O-Nef binding site to a region of the cytoplasmic tail of BST2, which is missing in short BST2, thus providing a rationale as to why O-Nefs do not antagonize short BST2 (21). Therefore, the absence of a physical association between O-Nef and short BST2 is likely to explain the lack of exclusion of short BST2 from virus budding sites and the almost undetectable levels of free cell surface BST2 capable of interacting with the pDC-inhibitory receptor ILT7. Consistent with these findings, the presence of O-Nefs in virus-producing cells did not induce BST2-dependent ILT7 activation or suppress IFN-I production by pDC-containing PBMCs during innate sensing of HIV-infected T cells. These findings highlight the crucial role of surface BST2 displacement in the modulation of the pDC IFN-I response via ILT7.

The lack of activation of the BST2/ILT7-dependent negative-feedback pathway by O-Nefs is expected to make infected cells more prone to triggering the release of IFN-I by pDCs during innate sensing. It is thus tempting to speculate that the absence of disease progression or effective control of pDC antiviral responses by HIV-1 group O strains during early stages following HIV transmission may have also contributed to their reduced transmission fitness. Indeed, studies in humanized mice demonstrated that the depletion of pDCs prior to HIV-1 infection prevented the induction of IFN-I and increased viral replication and dissemination (50). Furthermore, manipulation of IFN signaling in rhesus macaques during SIV transmission and acute infection via IFN receptor blockade or IFN-α2a administration was found to condition the local environment for the expression of antiviral genes and influence the establishment of systemic infection and disease progression (53). Enhanced IFN-I production by pDCs during the initial phase of infection is well known to condition the local environment for the expression of IFN-stimulating genes (including BST2), thus further affecting transmission fitness and viral spread *in vivo* (53).

The antiviral functions of BST2 go beyond simply restricting virus particle release and limiting viral spread in contexts where cell-free virus transmission is critical. It is also important to consider the role of BST2 in modulating many immune effector functions, including the control of IFN-I production by pDCs through ILT7, the activation of proinflammatory NF-κB signaling, as well as its effects on antibody opsonization. Clearly, a better understanding of the repertoire of BST2 antiviral activities and how these activities are counteracted by primate immunodeficiency virus antagonists will provide important insights into virus-host interactions governing viral transmission fitness and pathogenesis.

ACKNOWLEDGMENTS

We thank Fadi Hajjar for technical support; Robert Lodge, Scott Sugden, and Chris Leeks for helpful discussions; W. Todd Farmer for assistance and support with ImageJ analysis; E. Massicotte for assistance with flow cytometry; the IRCM clinic staff; and all volunteers for providing blood samples. The following reagents were obtained through the NIH AIDS Reagent Program: Sup-T1 from D. Ablashi, MT4 from D. Richman, and raltegravir (catalog number 11680) from Merck & Company, Inc.

FUNDING INFORMATION

This work was supported by Canadian Institutes of Health Research (CIHR) grant MOP-111226, by Canadian HIV Cure Enterprise grant HIG-133050 from the CIHR partnership with CANFAR and IAS, and by a grant from the Fonds de Recherche du Québec-Santé (FRQS) to E.A.C. E.A.C. is the recipient of the IRCM-Université de Montréal Chair of Excellence in HIV Research. F.K. is supported by grants from the Deutsche Forschungsgemeinschaft (DFG), a European FP7 Hit Hidden HIV grant (305762), and an Advanced ERC Investigator grant.

REFERENCES

1. **Kupzig S, Korolchuk V, Rollason R, Sugden A, Wilde A, Banting G.** 2003. Bst-2/HM1.24 is a raft-associated apical membrane protein with an unusual topology. Traffic **4:**694–709. http://dx.doi.org/10.1034/j.1600-0854.2003.00129.x.
2. **Neil SJ, Zang T, Bieniasz PD.** 2008. Tetherin inhibits retrovirus release and is antagonized by HIV-1 Vpu. Nature **451:**425–430. http://dx.doi.org/10.1038/nature06553.
3. **Van Damme N, Goff D, Katsura C, Jorgenson RL, Mitchell R, Johnson MC, Stephens EB, Guatelli J.** 2008. The interferon-induced protein BST-2 restricts HIV-1 release and is downregulated from the cell surface by the viral Vpu protein. Cell Host Microbe **3:**245–252. http://dx.doi.org/10.1016/j.chom.2008.03.001.
4. **Dave VP, Hajjar F, Dieng MM, Haddad E, Cohen EA.** 2013. Efficient BST2 antagonism by Vpu is critical for early HIV-1 dissemination in humanized mice. Retrovirology **10:**128. http://dx.doi.org/10.1186/1742-4690-10-128.
5. **Sato K, Misawa N, Fukuhara M, Iwami S, An DS, Ito M, Koyanagi Y.** 2012. Vpu augments the initial burst phase of HIV-1 propagation and downregulates BST2 and CD4 in humanized mice. J Virol **86:**5000–5013. http://dx.doi.org/10.1128/JVI.07062-11.
6. **Sauter D, Schindler M, Specht A, Landford WN, Munch J, Kim KA, Votteler J, Schubert U, Bibollet-Ruche F, Keele BF, Takehisa J, Ogando Y, Ochsenbauer C, Kappes JC, Ayouba A, Peeters M, Learn GH, Shaw G, Sharp PM, Bieniasz P, Hahn BH, Hatziioannou T, Kirchhoff F.** 2009. Tetherin-driven adaptation of Vpu and Nef function and the evolution of pandemic and nonpandemic HIV-1 strains. Cell Host Microbe **6:**409–421. http://dx.doi.org/10.1016/j.chom.2009.10.004.
7. **Pham TN, Lukhele S, Hajjar F, Routy JP, Cohen EA.** 2014. HIV Nef and Vpu protect HIV-infected $CD4^+$ T cells from antibody-mediated cell lysis through down-modulation of CD4 and BST2. Retrovirology **11:**15. http://dx.doi.org/10.1186/1742-4690-11-15.
8. **Arias JF, Heyer LN, von Bredow B, Weisgrau KL, Moldt B, Burton DR, Rakasz EG, Evans DT.** 2014. Tetherin antagonism by Vpu protects HIV-infected cells from antibody-dependent cell-mediated cytotoxicity. Proc Natl Acad Sci U S A **111:**6425–6430. http://dx.doi.org/10.1073/pnas.1321507111.
9. **Alvarez RA, Hamlin RE, Monroe A, Moldt B, Hotta MT, Rodriguez Caprio G, Fierer DS, Simon V, Chen BK.** 2014. HIV-1 Vpu antagonism of tetherin inhibits antibody-dependent cellular cytotoxic responses by natural killer cells. J Virol **88:**6031–6046. http://dx.doi.org/10.1128/JVI.00449-14.
10. **Galao RP, Le Tortorec A, Pickering S, Kueck T, Neil SJ.** 2012. Innate sensing of HIV-1 assembly by tetherin induces NFkappaB-dependent proinflammatory responses. Cell Host Microbe **12:**633–644. http://dx.doi.org/10.1016/j.chom.2012.10.007.
11. **Bego MG, Cote E, Aschman N, Mercier J, Weissenhorn W, Cohen EA.** 2015. Vpu exploits the cross-talk between BST2 and the ILT7 receptor to suppress anti-HIV-1 responses by plasmacytoid dendritic cells. PLoS Pathog **11:**e1005024. http://dx.doi.org/10.1371/journal.ppat.1005024.
12. **Cao W, Bover L, Cho M, Wen X, Hanabuchi S, Bao M, Rosen DB, Wang YH, Shaw JL, Du Q, Li C, Arai N, Yao Z, Lanier LL, Liu YJ.** 2009. Regulation of TLR7/9 responses in plasmacytoid dendritic cells by BST2 and ILT7 receptor interaction. J Exp Med **206:**1603–1614. http://dx.doi.org/10.1084/jem.20090547.
13. **Sharp PM, Hahn BH.** 2011. Origins of HIV and the AIDS pandemic. Cold Spring Harb Perspect Med **1:**a006841. http://dx.doi.org/10.1101/cshperspect.a006841.
14. **Sauter D, Specht A, Kirchhoff F.** 2010. Tetherin: holding on and letting go. Cell **141:**392–398. http://dx.doi.org/10.1016/j.cell.2010.04.022.
15. **Jia B, Serra-Moreno R, Neidermyer W, Rahmberg A, Mackey J, Fofana IB, Johnson WE, Westmoreland S, Evans DT.** 2009. Species-specific activity of SIV Nef and HIV-1 Vpu in overcoming restriction by tetherin/BST2. PLoS Pathog **5:**e1000429. http://dx.doi.org/10.1371/journal.ppat.1000429.
16. **Zhang F, Wilson SJ, Landford WC, Virgen B, Gregory D, Johnson MC, Munch J, Kirchhoff F, Bieniasz PD, Hatziioannou T.** 2009. Nef proteins

from simian immunodeficiency viruses are tetherin antagonists. Cell Host Microbe **6:**54–67. http://dx.doi.org/10.1016/j.chom.2009.05.008.
17. **Sauter D, Unterweger D, Vogl M, Usmani SM, Heigele A, Kluge SF, Hermkes E, Moll M, Barker E, Peeters M, Learn GH, Bibollet-Ruche F, Fritz JV, Fackler OT, Hahn BH, Kirchhoff F.** 2012. Human tetherin exerts strong selection pressure on the HIV-1 group N Vpu protein. PLoS Pathog **8:**e1003093. http://dx.doi.org/10.1371/journal.ppat.1003093.
18. **Le Tortorec A, Neil SJ.** 2009. Antagonism to and intracellular sequestration of human tetherin by the human immunodeficiency virus type 2 envelope glycoprotein. J Virol **83:**11966–11978. http://dx.doi.org/10.1128/JVI.01515-09.
19. **Vigan R, Neil SJ.** 2011. Separable determinants of subcellular localization and interaction account for the inability of group O HIV-1 Vpu to counteract tetherin. J Virol **85:**9737–9748. http://dx.doi.org/10.1128/JVI.00479-11.
20. **Yang SJ, Lopez LA, Exline CM, Haworth KG, Cannon PM.** 2011. Lack of adaptation to human tetherin in HIV-1 group O and P. Retrovirology **8:**78. http://dx.doi.org/10.1186/1742-4690-8-78.
21. **Kluge SF, Mack K, Iyer SS, Pujol FM, Heigele A, Learn GH, Usmani SM, Sauter D, Joas S, Hotter D, Bibollet-Ruche F, Plenderleith LJ, Peeters M, Geyer M, Sharp PM, Fackler OT, Hahn BH, Kirchhoff F.** 2014. Nef proteins of epidemic HIV-1 group O strains antagonize human tetherin. Cell Host Microbe **16:**639–650. http://dx.doi.org/10.1016/j.chom.2014.10.002.
22. **Mourez T, Simon F, Plantier JC.** 2013. Non-M variants of human immunodeficiency virus type 1. Clin Microbiol Rev **26:**448–461. http://dx.doi.org/10.1128/CMR.00012-13.
23. **Cocka LJ, Bates P.** 2012. Identification of alternatively translated tetherin isoforms with differing antiviral and signaling activities. PLoS Pathog **8:**e1002931. http://dx.doi.org/10.1371/journal.ppat.1002931.
24. **Neil SJ.** 2013. The antiviral activities of tetherin. Curr Top Microbiol Immunol **371:**67–104. http://dx.doi.org/10.1007/978-3-642-37765-5_3.
25. **Zhang F, Landford WN, Ng M, McNatt MW, Bieniasz PD, Hatziioannou T.** 2011. SIV Nef proteins recruit the AP-2 complex to antagonize tetherin and facilitate virion release. PLoS Pathog **7:**e1002039. http://dx.doi.org/10.1371/journal.ppat.1002039.
26. **Serra-Moreno R, Zimmermann K, Stern LJ, Evans DT.** 2013. Tetherin/BST-2 antagonism by Nef depends on a direct physical interaction between Nef and tetherin, and on clathrin-mediated endocytosis. PLoS Pathog **9:**e1003487. http://dx.doi.org/10.1371/journal.ppat.1003487.
27. **Lau D, Kwan W, Guatelli J.** 2011. Role of the endocytic pathway in the counteraction of BST-2 by human lentiviral pathogens. J Virol **85:**9834–9846. http://dx.doi.org/10.1128/JVI.02633-10.
28. **Weinelt J, Neil SJ.** 2014. Differential sensitivities of tetherin isoforms to counteraction by primate lentiviruses. J Virol **88:**5845–5858. http://dx.doi.org/10.1128/JVI.03818-13.
29. **McNatt MW, Zang T, Bieniasz PD.** 2013. Vpu binds directly to tetherin and displaces it from nascent virions. PLoS Pathog **9:**e1003299. http://dx.doi.org/10.1371/journal.ppat.1003299.
30. **Lewinski MK, Jafari M, Zhang H, Opella SJ, Guatelli J.** 2015. Membrane anchoring by a C-terminal tryptophan enables HIV-1 Vpu to displace bone marrow stromal antigen 2 (BST2) from sites of viral assembly. J Biol Chem **290:**10919–10933. http://dx.doi.org/10.1074/jbc.M114.630095.
31. **Pujol FM, Laketa V, Schmidt F, Mukenhirn M, Muller B, Boulant S, Grimm D, Keppler OT, Fackler OT.** 2016. HIV-1 Vpu antagonizes CD317/tetherin by adaptor protein-1-mediated exclusion from virus assembly sites. J Virol **90:**6709–6723. http://dx.doi.org/10.1128/JVI.00504-16.
32. **Bego MG, Dube M, Mercier J, Cohen EA.** 2009. Effect of calcium-modulating cyclophilin ligand on human immunodeficiency virus type 1 particle release and cell surface expression of tetherin. J Virol **83:**13032–13036. http://dx.doi.org/10.1128/JVI.01786-09.
33. **Dube M, Roy BB, Guiot-Guillain P, Binette J, Mercier J, Chiasson A, Cohen EA.** 2010. Antagonism of tetherin restriction of HIV-1 release by Vpu involves binding and sequestration of the restriction factor in a perinuclear compartment. PLoS Pathog **6:**e1000856. http://dx.doi.org/10.1371/journal.ppat.1000856.
34. **Dube M, Paquay C, Roy BB, Bego MG, Mercier J, Cohen EA.** 2011. HIV-1 Vpu antagonizes BST-2 by interfering mainly with the trafficking of newly synthesized BST-2 to the cell surface. Traffic **12:**1714–1729. http://dx.doi.org/10.1111/j.1600-0854.2011.01277.x.
35. **Zazopoulos E, Haseltine WA.** 1992. Mutational analysis of the human immunodeficiency virus type 1 Eli Nef function. Proc Natl Acad Sci U S A **89:**6634–6638. http://dx.doi.org/10.1073/pnas.89.14.6634.
36. **Ablashi DV, Berneman ZN, Kramarsky B, Whitman J, Jr, Asano Y, Pearson GR.** 1995. Human herpesvirus-7 (HHV-7): current status. Clin Diagn Virol **4:**1–13. http://dx.doi.org/10.1016/0928-0197(95)00005-S.
37. **Cao W, Rosen DB, Ito T, Bover L, Bao M, Watanabe G, Yao Z, Zhang L, Lanier LL, Liu YJ.** 2006. Plasmacytoid dendritic cell-specific receptor ILT7-Fc epsilonRI gamma inhibits Toll-like receptor-induced interferon production. J Exp Med **203:**1399–1405. http://dx.doi.org/10.1084/jem.20052454.
38. **Dube M, Roy BB, Guiot-Guillain P, Mercier J, Binette J, Leung G, Cohen EA.** 2009. Suppression of tetherin-restricting activity upon human immunodeficiency virus type 1 particle release correlates with localization of Vpu in the trans-Golgi network. J Virol **83:**4574–4590. http://dx.doi.org/10.1128/JVI.01800-08.
39. **Bego MG, Mercier J, Cohen EA.** 2012. Virus-activated interferon regulatory factor 7 upregulates expression of the interferon-regulated BST2 gene independently of interferon signaling. J Virol **86:**3513–3527. http://dx.doi.org/10.1128/JVI.06971-11.
40. **Usami Y, Wu Y, Gottlinger HG.** 2015. SERINC3 and SERINC5 restrict HIV-1 infectivity and are counteracted by Nef. Nature **526:**218–223. http://dx.doi.org/10.1038/nature15400.
41. **Rosa A, Chande A, Ziglio S, De Sanctis V, Bertorelli R, Goh SL, McCauley SM, Nowosielska A, Antonarakis SE, Luban J, Santoni FA, Pizzato M.** 2015. HIV-1 Nef promotes infection by excluding SERINC5 from virion incorporation. Nature **526:**212–217. http://dx.doi.org/10.1038/nature15399.
42. **Lepelley A, Louis S, Sourisseau M, Law HK, Pothlichet J, Schilte C, Chaperot L, Plumas J, Randall RE, Si-Tahar M, Mammano F, Albert ML, Schwartz O.** 2011. Innate sensing of HIV-infected cells. PLoS Pathog **7:**e1001284. http://dx.doi.org/10.1371/journal.ppat.1001284.
43. **Bush S, Tebit DM.** 2015. HIV-1 group O origin, evolution, pathogenesis, and treatment: unraveling the complexity of an outlier 25 years later. AIDS Rev **17:**147–158.
44. **Nkengasong JN, Fransen K, Willems B, Karita E, Vingerhoets J, Kestens L, Colebunders R, Piot P, van der Groen G.** 1997. Virologic, immunologic, and clinical follow-up of a couple infected by the human immunodeficiency virus type one, group O. J Med Virol **51:**202–209.
45. **Mas A, Quinones-Mateu E, Soriano V, Domingo E.** 1996. Env gene characterization of the first HIV type 1 group O Spanish isolate. AIDS Res Hum Retroviruses **12:**1647–1649. http://dx.doi.org/10.1089/aid.1996.12.1647.
46. **Dittmar MT, Zekeng L, Kaptue L, Eberle J, Krausslich HG, Gurtler L.** 1999. Coreceptor requirements of primary HIV type 1 group O isolates from Cameroon. AIDS Res Hum Retroviruses **15:**707–712. http://dx.doi.org/10.1089/088922299310791.
47. **Buckheit RW, III, Sexauer SB, Sedaghat AR, Wilke CO, Laeyendecker O, Basseth CR, Blankson JN.** 2014. Long-term control of viral replication in a group O, human immunodeficiency virus type 1-infected individual. AIDS Res Hum Retroviruses **30:**511–513. http://dx.doi.org/10.1089/aid.2014.0054.
48. **Arien KK, Abraha A, Quinones-Mateu ME, Kestens L, Vanham G, Arts EJ.** 2005. The replicative fitness of primary human immunodeficiency virus type 1 (HIV-1) group M, HIV-1 group O, and HIV-2 isolates. J Virol **79:**8979–8990. http://dx.doi.org/10.1128/JVI.79.14.8979-8990.2005.
49. **Haase AT.** 2010. Targeting early infection to prevent HIV-1 mucosal transmission. Nature **464:**217–223. http://dx.doi.org/10.1038/nature08757.
50. **Li G, Cheng M, Nunoya J, Cheng L, Guo H, Yu H, Liu YJ, Su L, Zhang L.** 2014. Plasmacytoid dendritic cells suppress HIV-1 replication but contribute to HIV-1 induced immunopathogenesis in humanized mice. PLoS Pathog **10:**e1004291. http://dx.doi.org/10.1371/journal.ppat.1004291.
51. **Jia X, Weber E, Tokarev A, Lewinski M, Rizk M, Suarez M, Guatelli J, Xiong Y.** 2014. Structural basis of HIV-1 Vpu-mediated BST2 antagonism via hijacking of the clathrin adaptor protein complex 1. eLife **3:**e02362. http://dx.doi.org/10.7554/eLife.02362.
52. **Kueck T, Foster TL, Weinelt J, Sumner JC, Pickering S, Neil SJ.** 2015. Serine phosphorylation of HIV-1 Vpu and its binding to tetherin regulates interaction with clathrin adaptors. PLoS Pathog **11:**e1005141. http://dx.doi.org/10.1371/journal.ppat.1005141.
53. **Sandler NG, Bosinger SE, Estes JD, Zhu RT, Tharp GK, Boritz E, Levin D, Wijeyesinghe S, Makamdop KN, del Prete GQ, Hill BJ, Timmer JK, Reiss E, Yarden G, Darko S, Contijoch E, Todd JP, Silvestri G, Nason M, Norgren RB, Jr, Keele BF, Rao S, Langer JA, Lifson JD, Schreiber G, Douek DC.** 2014. Type I interferon responses in rhesus macaques prevent SIV infection and slow disease progression. Nature **511:**601–605. http://dx.doi.org/10.1038/nature13554.